Available online at www.sciencedirect.com
SCIENCE DIRECT
Journal of Organometallic Chemistry 691 (2006) 1780–1789
Journal of Organometallic Chemistry
www.elsevier.com/locate/jorganchem

Synthesis and characterization of a new chloro-di-phenyltin(IV) complex with 2-mercapto-nicotinic acid: Study of its influence upon the catalytic oxidation of linoleic acid to hydroperoxylinoleic acid by the enzyme lipoxygenase

Marianna N. Xanthopoulou [a], Sotiris K. Hadjikakou [a,*], Nick Hadjiliadis [a,*], Maciej Kubicki [b], Spyros Karkabounas [c], Konstantinos Charalabopoulos [c], Nikolaos Kourkoumelis [d], Thomas Bakas [d]

[a] *Inorganic and Analytical Chemistry, Department of Chemistry, University of Ioannina, 45110 Ioannina, Greece*
[b] *Department of Chemistry, A. Mickiewicz, University, ul. Grunwaldzka 6, 60-780 Poznan, Poland*
[c] *Department of Experimental Physiology, Medical School, University of Ioannina, 45110 Ioannina, Greece*
[d] *Physics of Material Laboratory, Department of Physics, University of Ioannina, 45110 Ioannina, Greece*

Received 24 November 2005; accepted 28 November 2005
Available online 3 February 2006

Abstract

The complex $[(C_6H_5)_2SnCl(HMNA)]$ (**1**) where H_2MNA is thioamide 2-mercapto-nicotinic acid has been synthesized by reacting a methanolic solution of di-chloro-di-phenyltin(IV) Ph_2SnCl_2 with an aqueous solution of 2-mercapto-nicotinic acid, containing twofold amount of potassium hydroxide. The Sn/ligand molar ratio is 2:1. The complex was characterized by elemental analysis, FT-IR and Mössbauer spectroscopic techniques. In addition the crystal structure of the molecule was determined by an X-ray diffraction at 293(2) K. $C_{18}H_{14}ClNO_2SSn$ is monoclinic, space group $P2_1/n$, $a = 15.089(3)$ Å, $b = 15.846(3)$ Å, $c = 16.691(3)$ Å, $\beta = 105.57(3)°$, $Z = 8$. The ligand coordinates to the metal center through the exocyclic sulfur and the heterocyclic nitrogen atoms, forming a four membered ring. The coordination sphere around the tin(IV) ion is completed with two carbon atoms from the two phenyl groups and one chlorine atom. The geometry around the tin atom can be described either as trigonal bipyramidal or tetragonal pyramidal. Finally, the influence of the complex $[(C_6H_5)_2SnCl(HMNA)]$ (**1**) upon the catalytic peroxidation of linoleic acid to hydroperoxylinoleic acid by the enzyme lipoxygenase (LOX) was also kinetically and theoretically studied and the results compared with the ones of the corresponding binuclear complex $[(C_6H_5)_3Sn(MNA)Sn(C_6H_5)_3 \cdot (acetone)]$ (**2**) reported in the literature.

Keywords: Bioinorganic chemistry; Organotin(IV) compounds; S ligands; Heterocyclic thioamides; Crystal structures

1. Introduction

The biological activity of organotin(IV) compounds is well known [1–3]. Most organotin(IV) compounds are generally toxic [3]. The binding of organotins by thiol groups, on the other hand, is significant in biological systems [4,5]. Although the anti-tumour activity of many organotin(IV) compounds has already been identified, the precise mechanism of this activity is still a matter of investigation [1,2]. Today, a number of organotin(IV) derivatives are known to have an efficient anti-tumour activity [6]. A comparison of the structures of the active and inactive compounds suggests that all active compounds should conform to the

* Corresponding authors. Tel.: +30 26510 98374 (S.K. Hadjikakou), Tel.: +30 26510 98420; fax: +30 26510 44831 (N. Hadjiliadis).
E-mail addresses: shadjika@cc.uoi.gr (S.K. Hadjikakou), nhadjis@cc.uoi.gr (N. Hadjiliadis).

0022-328X/$ - see front matter © 2005 Elsevier B.V. All rights reserved.
doi:10.1016/j.jorganchem.2005.11.073

following requirements: (i) to have available coordination positions around Sn and (ii) to have a relatively stable ligand–Sn bond (e.g., Sn–N and Sn–S) with low hydrolytic decomposition [7]. Organotin(IV) complexes with thioamides have also been synthesized and studied for their anti-tumor activity [8–27]. We recently studied the synthesis, structural characterization and in vitro cytotoxicity of organotin(IV) derivatives of the heterocyclic thioamides, 2-mercaptobenzothiazole, 5-chloro-2-mercaptobenzothiazole, 3-methyl-2-mercaptobenzothiazole and 2-mercaptonicotinic acid [5a,5b]. The significantly strong anticancer activity evaluated for the tri-organotin(IV) derivatives is attributed to the availability of coordination sites due to trigonal bipyramidal geometry around the tin(IV) ion, while the milder anti-tumor activity shown by di-organotin(IV) compounds can be ascribed to the non-availability of such coordination sites due to the six coordinated tin(IV) ions [27].

On the other hand, it is well known that the interaction of heavy metals with free sulfhydryl groups in proteins and therefore the distortion of the protein structure is one of the proposed mechanisms of the metal-induced cell death [5c,28]. The possibility of organotins to deplete HS-groups in proteins is however restricted when the organotin complexes posses the S-bonded ligands as 2-mercapto-nicotinic acid. This prompted us to investigate the enzyme inhibitions by organotin(IV) complexes. Lipoxygenase (LOX) is an enzyme which catalyzes the oxidation of arachidonic acid to leukotrienes, in an essential mechanism for the cell life [29].

Complex $[(C_6H_5)_2SnCl(HMNA)]$ (**1**), reported here and the binuclear derivative $[(C_6H_5)_3Sn(MNA)Sn(C_6H_5)_3 \cdot (acetone)]$ (**2**) already reported [5a,5b] were used to study the influence on the catalytic peroxidation of linoleic acid to hydroperoxylinoleic acid by the enzyme lipoxygenase (LOX), both kinetically and theoretically.

2. Results and discussion

2.1. General aspects

Complex **1** was synthesized by reacting a methanolic solution of di-phenyltin(IV) di-chloride $(C_6H_5)_2SnCl_2$ with an aqueous solution of the 2-mercapto-nicotinic acid (H_2MNA). The Sn/ligand/KOH molar ratio was 2:1:2. The reaction taking place is shown below

$$P(C_6H_5)_2SnCl_2 + H_2MNA \xrightarrow{KOH} (C_6H_5)_2SnCl(MNAH) + KCl + H_2O$$

^1H, ^{13}C NMR and FT-IR spectroscopic data of the complex prepared here confirmed the proposed molecular formula. Compound **1** is an air stable powder. Crystals of **1** suitable for X-ray analysis were obtained by slow evaporation of dichloromethane solutions.

2.2. Spectroscopy

2.2.1. Vibrational spectroscopy

The IR spectrum of the complex shows distinct vibrational bands at 1565 and 1390 cm^{-1}, which can be assigned to ν(CN) vibrations (thioamide I and II bands) and at 1077 and 664 cm^{-1}, which can be attributed to the ν(CS) vibrations (thioamide III and IV bands). No bands due to the ν(NH) or ν(SH) vibrations are observed in the IR spectrum of the complex, indicating the deprotonation of all ligands. The corresponding thioamide vibration bands are observed at 1562, 1310, 1071 and 650 cm^{-1} for the ligand [5a]. Thioamide bands are shifted to higher frequencies in the complex, supporting both sulfur donation and deprotonation of the ligands. The band at 383 cm^{-1} is attributed to the ν(Sn–S) vibrations, while bands at 255 and 205 cm^{-1} are assigned to the ν(Sn–N) [5a,30]. The ν(Sn–Cl) vibrations are observed at 282 and 221 cm^{-1} [31].

2.2.2. ^{119}Sn Mössbauer spectroscopy

Solid state ^{119}Sn Mössbauer spectroscopic data of complexes **1** and the known **2** are given in Table 1

The spectra of compounds **1** and **2**, recorded at 80 and 85 K, respectively, consist of two symmetrical Lorentzian doublets, which indicate the presence of two tin atoms as a result of the presence of two independent molecules in the unit cell in case of **1** (see crystal structure) and in the presence of two tin(IV) ions in complex **2** [5a]. The values of the isomer shift parameters, δ, (1.276 and 0.656 mm s^{-1} for **1** and 1.290 and 1.232 mm s^{-1} for **2**) lie in the region for $R_2Sn(IV)$ species [2,23,32]. The quadrupole splitting values (QS) of both doublets (2.642 mm s^{-1} and 2.172 mm s^{-1} for **1** and 2.895 and 1.414 mm s^{-1} for **2**) correspond to a distorted trigonal bipyramidal geometry around both tin atoms in case of **1** and to trigonal bipyramidal for the one atom of complex **2** and to a tetrahedral geometry for the other [32], despite the crystal structure of **2** showing a trigonal bipyramidal arrangement, around both tin atoms [5a,5b].

2.3. Crystal and molecular structure of $[(C_6H_5)_2SnCl(HMNA)]$ (1)

Crystal structure of complex **1** was determined at 293(2) K. Fig. 1 gives an ORTEP diagram of the complex.

Table 1
^{119}Sn Mössbauer spectroscopic data for complexes **1**–**2**

Complexes	Temperature (K)	δ (mm s^{-1})	QS (mm s^{-1})	Area (%)	δ (mm s^{-1})	QS (mm s^{-1})	Area (%)
1	80	1.276	2.642	59	0.656	2.172	41
2	85	1.290	2.895	55	1.232	1.414	45

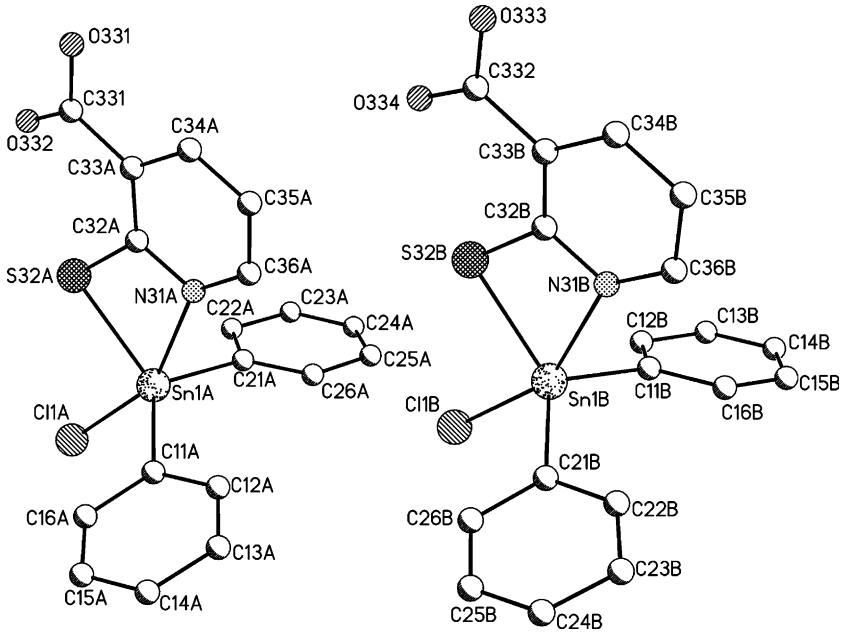

Fig. 1. ORTEP diagram of molecule **1** together with the atomic numbering scheme. There are two independent molecules in the unit cell.

Selected bond distances and bond angles are given in Table 2.

There are two independent molecules in the unit cell (**1A**) and (**1B**). Compound **1** is a covalent monomer in the solid state with a distorted trigonal bipyramidal or tetragonal pyramidal geometry around the metal ions, based on Reedijk's criteria [33]. According to Reedijk [33] when the parameter $\tau = (\beta - \alpha)/60$ equals zero a tetragonal pyramidal structure is obtained, while in trigonal bipyramidal structure equals to unity (Scheme 1). In our case $\beta = 155.43°$ and $\alpha = 123.8°$ for (**1A**) and $\beta = 154.96°$ and $\alpha = 119.5°$ for (**1B**) complexes, respectively. Therefore, $\tau = 0.53$ for (**1A**) and $\tau = 0.59$ for (**1B**). Taking in to account the Mossbauer results a trigonal bipyramidal structure may be postulate.

Two phenyl-groups are bonded to the tin ion (Sn(1A)–C(21A) = 2.103(8), Sn(1A)–C(11A) = 2.107(7) Å, respectively, for (**1A**) and Sn(1B)–C(21B) = 2.102(8) and Sn(1B)–C(11B) = 2.120(7) Å, respectively, for (**1B**)). One deprotonated thioamide ligand is also bonded to the tin atom via sulphur (Sn(1A)–S(32A) = 2.4383(17), Sn(1B)–S(32B) = 2.4396(18) Å in (**1A**) and (**1B**), respectively). The Sn–S bond distances of (**1A**) and (**1B**) are shorter than the corresponding distances found in the $[(C_6H_5)_2SnCl$-

Table 2
Selected bond lengths (Å) and bond angles (°) for complex **1** with e.s.d.'s in parentheses

Complex (**1A**)		Complex (**1B**)	
(a) Bond lengths (Å)			
Sn(1A)–C(21A)	2.103(8)	Sn(1B)–C(21B)	2.102(8)
Sn(1A)–C(11A)	2.107(7)	Sn(1B)–C(11B)	2.120(7)
Sn(1A)–Cl(1A)	2.4246(19)	Sn(1B)–Cl(1B)	2.424(2)
Sn(1A)–N(31A)	2.435(5)	Sn(1B)–S(32B)	2.4396(18)
Sn(1A)–S(32A)	2.4383(17)	Sn(1B)–N(31B)	2.441(5)
C(32A)–S(32A)	1.750(6)	C(32B)–S(32B)	1.753(6)
N(31A)–C(32A)	1.343(7)	N(31B)–C(36B)	1.327(8)
N(31A)–C(36A)	1.345(8)	N(31B)–C(32B)	1.346(7)
(b) Bond angles (°)			
C(21A)–Sn(1A)–C(11A)	123.8(3)	C(21B)–Sn(1B)–C(11B)	119.5(3)
C(21A)–Sn(1A)–Cl(1A)	102.2(2)	C(21B)–Sn(1B)–Cl(1B)	100.2(2)
C(11A)–Sn(1A)–Cl(1A)	98.87(18)	C(11B)–Sn(1B)–Cl(1B)	102.04(18)
C(21A)–Sn(1A)–N(31A)	91.2(2)	C(21B)–Sn(1B)–S(32B)	118.31(19)
C(11A)–Sn(1A)–N(31A)	90.4(2)	C(11B)–Sn(1B)–S(32B)	116.59(18)
Cl(1A)–Sn(1A)–N(31A)	155.43(13)	Cl(1B)–Sn(1B)–S(32B)	91.26(7)
C(21A)–Sn(1A)–S(32A)	109.5(2)	C(21B)–Sn(1B)–N(31B)	90.9(2)
C(11A)–Sn(1A)–S(32A)	121.08(17)	C(11B)–Sn(1B)–N(31B)	91.6(2)
Cl(1A)–Sn(1A)–S(32A)	92.22(7)	Cl(1B)–Sn(1B)–N(31B)	154.96(13)
N(31A)–Sn(1A)–S(32A)	63.69(12)	S(32B)–Sn(1B)–N(31B)	63.77(12)

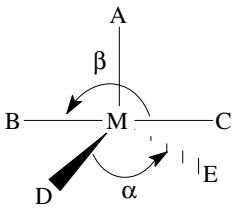

Scheme 1.

(mbzt)] (Sn–S = 2.473(2) Å, where mbzt = 2-mercapto-benzothiazole) [11], in [$(C_2H_5)_2$SnBr(TNiPE)] (Sn–S = 2.462(3) Å, where TNiPE = *iso*-propyl ester of 2-mercapto-nicotinic acid) [8], in [$(CH_3)_2$SnCl(TNEE)] (Sn–S = 2.473(2) Å, where TNEE = ethyl ester of 2-mercapto-nicotinic acid) [8], in [(*n*-$C_4H_9)_2$Sn(mbzt)$_2$] (Sn–S = 2.500(2), 2.5092(19) Å, where mbzt = 2-mercapto-benzothiazole) [5a], in [$(CH_3)_2$Sn(cmbzt)$_2 \cdot (H_2O)$] (Sn–S = 2.494(4), 2.509(4) Å, where cmbzt = 5 chloro-2-mercapto-benzothiazole) [5a]. The geometry around the metal center is completed by strong Sn–N bonding interaction between the nitrogen atoms of the ligand and the metal center (Sn(1A)–N(31A) = 2.435(5), Sn(1B)–N(31B) = 2.441(5) Å in (**1A**) and (**1B**), respectively). The Sn–N bond distances found in (**1A**) and (**1B**) are among the shortest measured for such complexes [$(C_6H_5)_2$SnCl(mbzt)] (Sn–N = 2.405(7) Å, where mbzt = 2-mercapto-benzothiazole) [11], in [$(C_2H_5)_2$SnBr(TNiPE)] (Sn–N = 2.488(9) Å, where TNiPE = *iso*-propyl ester of 2-mercapto-nicotinic acid) [8], in [$(CH_3)_2$SnCl(TNEE)] (Sn–N = 2.426(4) Å, where TNEE = ethyl ester of 2-mercapto-nicotinic acid) [8], in [(*n*-$C_4H_9)_2$-Sn(mbzt)$_2$] (Sn–N = 2.730(5), 2.780(6) Å, where mbzt = 2-mercapto-benzothiazole) [5a], in [$(CH_3)_2$Sn(cmbzt)$_2 \cdot$ (H_2O)] (Sn–N = 2.635, 2.802 Å, where cmbzt = 5 chloro-2-mercapto-benzothiazole) [5a].

An inter-molecular hydrogen bonding is also formed between the carboxylic groups (Fig. 2) (O331–H331···O332 = 1.8861 Å, O331···O332 = 2.701(7) Å and ∠H331–O331···O332 = 173.49° and H333[O334]···O333 = 1.8767 Å, O333···O334 = 2.694(7) Å and ∠O333–H333···O334 = 173.88°).

*2.4. Study of the peroxidation of linoleic acid by the enzyme of lipoxygenase (LOX) in the presence of complexes **1** and **2***

The influence of complexes **1** and **2** on the oxidation of the linoleic acid by the enzyme LOX was studied in a wide concentration range. Fig. 3 compares the inhibitory effect of the complexes **1** and **2** in various concentrations. It is shown that the catalytic activity of LOX decreased significantly in the presence of low concentrations (about 5–75 μM) of both complexes **1** and **2**. The degree of LOX activity (**A** %) in the presence of the complexes was calculated according to the following equation [34]:

$$\mathbf{A}\ (\%) = \left(\frac{\upsilon_0 \text{ in the presence of inhibitor}}{\upsilon_0 \text{ in the absence of inhibitor}}\right) \times 100\ (\%)$$

where υ_0 is the initial rate.

The value of the initial rate (υ_0, μM min^{-1}) was calculated according to the following formula:

$$\upsilon_0 = \frac{\Delta C}{\Delta t} = \frac{\Delta A}{\Delta t \varepsilon} = \frac{tg\alpha}{\varepsilon}$$

where C is the product concentration (hypedroperoxy-linoleic acid), t is the reaction time, ε molar absorbance coefficient of hypedroperoxy-linoleic acid, $tg\alpha$ is the slope of the kinetic curve plotted as absorbance vs. time.

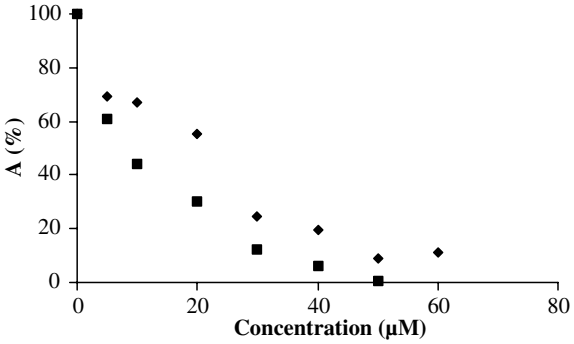

Fig. 3. Inhibitory effect of the complexes **1** (◆) and **2** (■) in various concentrations.

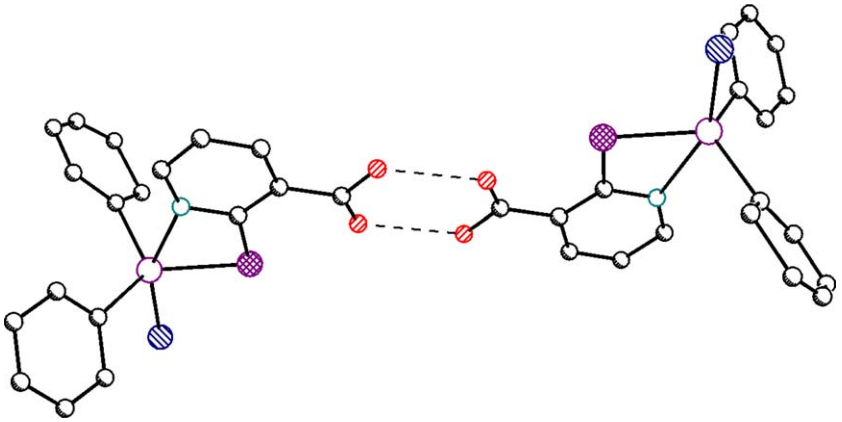

Fig. 2. Intra-molecular linkages via O–H···O interactions in compound **1**.

The IC_{50} values indicate higher inhibitory activity of complex **2** than **1** (14 and 26 μM, respectively) and they depend on the number of phenyl groups in the molecules and the number of tin atoms.

In order to evaluate the inhibition type, the enzymatic reaction was studied by steady-state kinetics in various substrate's concentrations (varied from 0.01 to 0.1 mM) in the absence and presence of the complexes (15 μM). The experimental data were processed by graphical method in Lineweaver-Burk coordinates (double reciprocal method). The kinetic parameters were estimated from the slope and intercept of the line. The K_m of the enzyme is 0.035 mM with υ_{max} of 27.5 mM/s, while the corresponding apparent values for complexes **1** and **2** are found to be 0.078 and 0.060 mM with υ_{max} values 25.8 and 13.33 mM/s, respectively. Thus, the studied compounds inhibit the enzyme with a reversible mixed inhibition mechanism [35]. In this mechanism both the EI (enzyme–inhibitor) and ESI (enzyme–substrate–inhibitor) complexes are formed [35]. This occurs when the inhibitor binds at a site away from the substrate binding site, causing a reduction in the catalytic rate.

2.5. Computational methods – docking study

The level of LOX inhibitory effect activities of compounds **1** and **2** prompted us to perform molecular docking studies to understand the complex–protein interactions. The binding energy (E) of the substrate (S = linoleic acid) to its binding site in the enzyme LOX (E) when **ES** complex formed is $E = -7.89$ kcal/mol. The corresponding binding energies of inhibitors (I), in **ESI** are calculated to −8.27 **1** and −8.69 **2** kcal/mol, respectively, while the binding energies of **EI** are found to be −8.28 **1** and −9.63 **2** kcal/mol. According to the E values of **ES** in contrast to those of **EI** and **ESI** indicate that both **ESI** and **EI** complexes could be formed.

The substrate binding site in **ES** is located away from the active site of LOX (d(Fe–C) = 19.7, d(Fe–C) = 21.4 Å) and it is found to pose in 76ALA, 533ARG, 760ASP, 761GLU, 249LEU, 110LYS, 15MET, 108PHE, 759SER and 762VAL (Fig. 4). The docked conformations of the two complexes **1** and **2** in **EI** complex are located away from the active site of LOX. The calculated distances between inhibitor's tin(IV) ions and the iron of the active site of the enzyme LOX in **EI** complexes are found to be d(Fe–Sn) = 24.7 Å in case of **1** and d(Fe–Sn1) = 24.2 Å and d(Fe–Sn2) = 26.5 Å in case of **2**. The 'walls' of this binding pocket in case of complex **1** consist of the amino acid residues: 76ALA, 18ASN, 77GLY, 247GLY, 248HIS, 249LEU, 17LYS, 15MET, 108PHE, 16PRO and 130TRP, while in case of **2** consist of the amino acid residues: 18ASN, 75GLY, 77GLY, 248HIS, 249LEU, 250LYS, 252LYS, 15MET, 108PHE, 16PRO and 251SER. Fig. 5 shows ribbon representation of complex **1** (Fig. 5A) and complex **2** (Fig. 5B) docked into the binding site of the enzyme LOX in case of **EI**. The corresponding docked conformations of the two complexes **1** and **2** in the **ESI** complex are also located away from the active site of LOX as well as from the substrate binding site. The calculated distances between inhibitor's tin(IV) ions and the iron of the active site of the enzyme LOX in **ESI** complexes are found to be d(Fe–Sn) = 24.7 Å in case of **1** and d(Fe–Sn1) = 24.2 Å and d(Fe–Sn2) = 26.0 Å in case

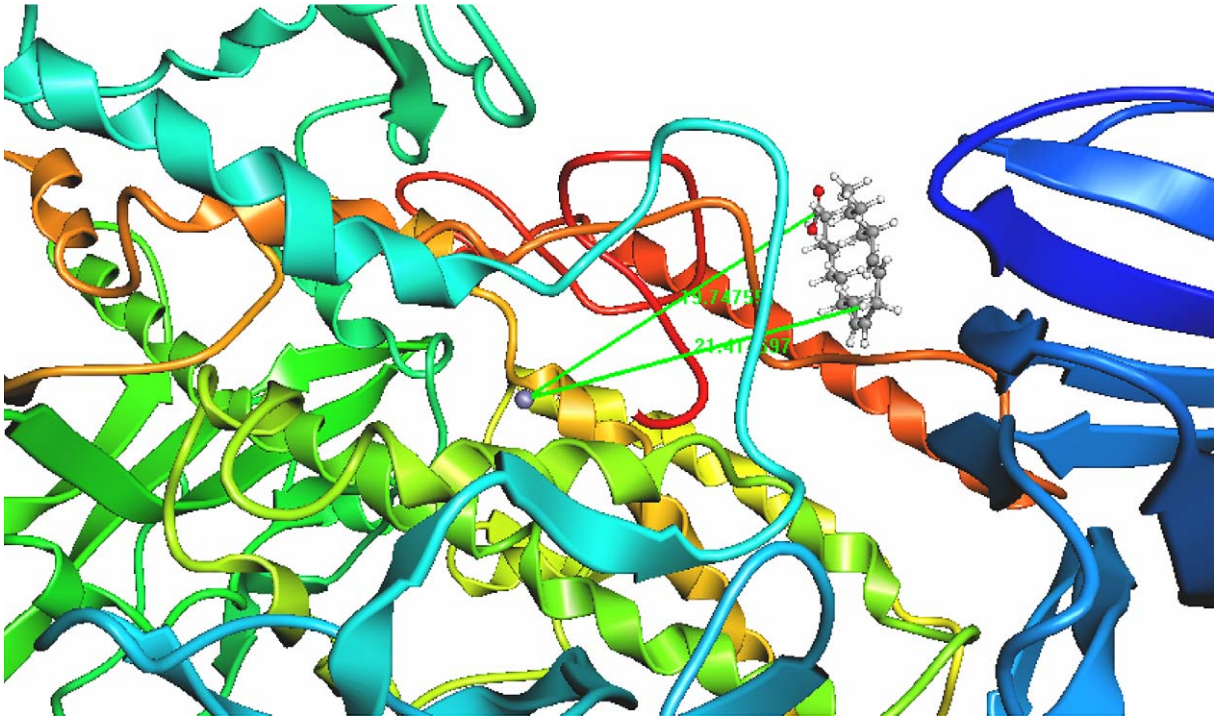

Fig. 4. Ribbon representation of the substrate docked into the binding site of the enzyme LOX (**ES**).

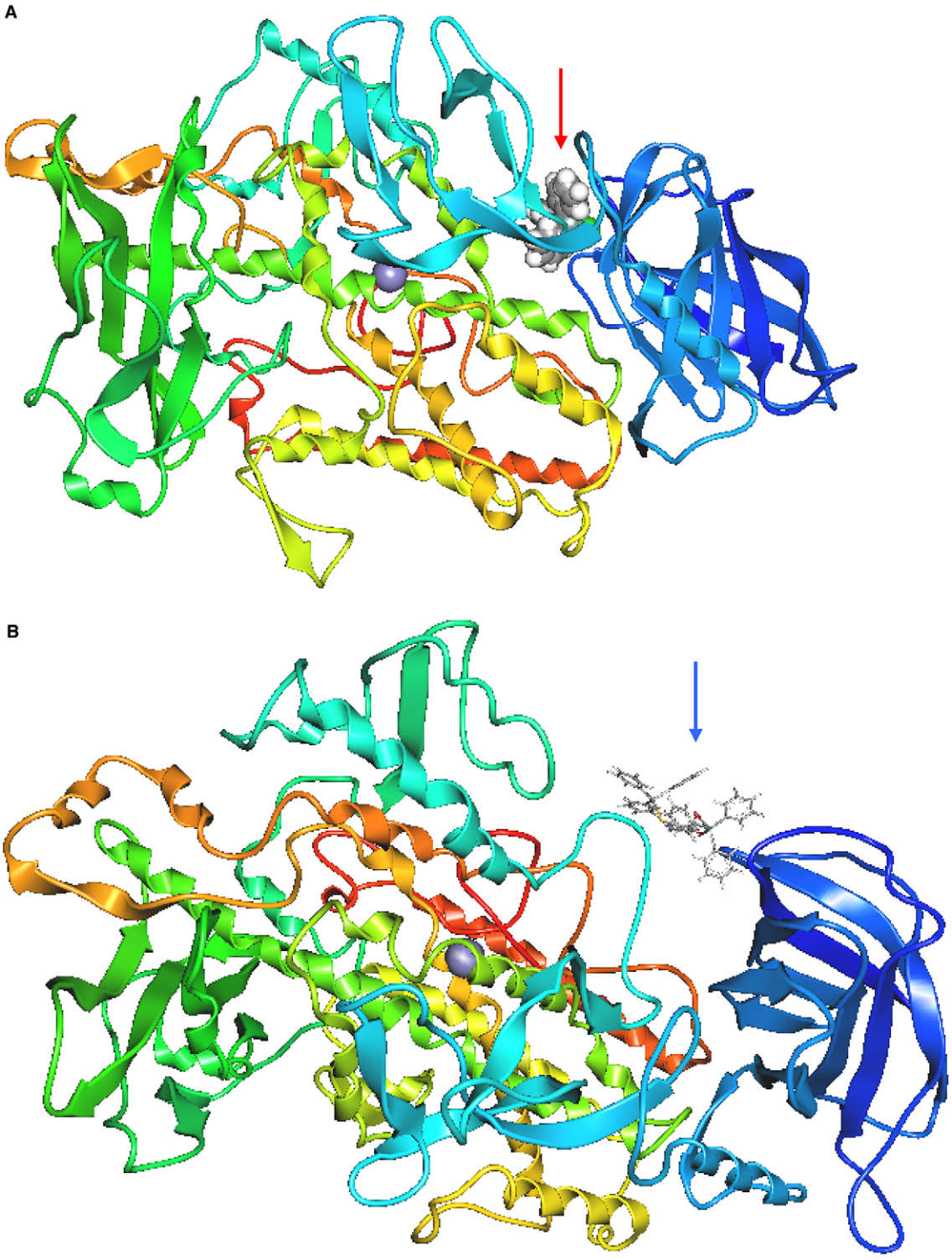

Fig. 5. Ribbon representation of the complexes **1** (A) and **2** (B) docked into the binding site of the enzyme LOX (**EI**).

of (**2**), while the shortest distances between inhibitor's tin(IV) atoms and linoleic acid (substrate) are found to be 4.41 Å in case of (**1**) and 7.48 and 6.91 Å, respectively, in case of **2**. The 'walls' of this binding pocket in case of complex **1** in **ESI** consist of the same amino acid residues as in case of complex **EI** (Fig. 6A), while in case of **2** consist of the amino acid residues: 76ALA, 18ASN, 78GLU, 75GLY, 77GLY, 248HIS, 249LEF, 250LYS, 252LYS, 15MET and 251SER (Fig. 6B).

Thus, according to computational studies, inhibitor binds to a site away from the substrate binding site while both **ESI** and **EI** complexes could be formed. These findings further support the reversible mixed inhibition mechanism which were also found from kinetic studies.

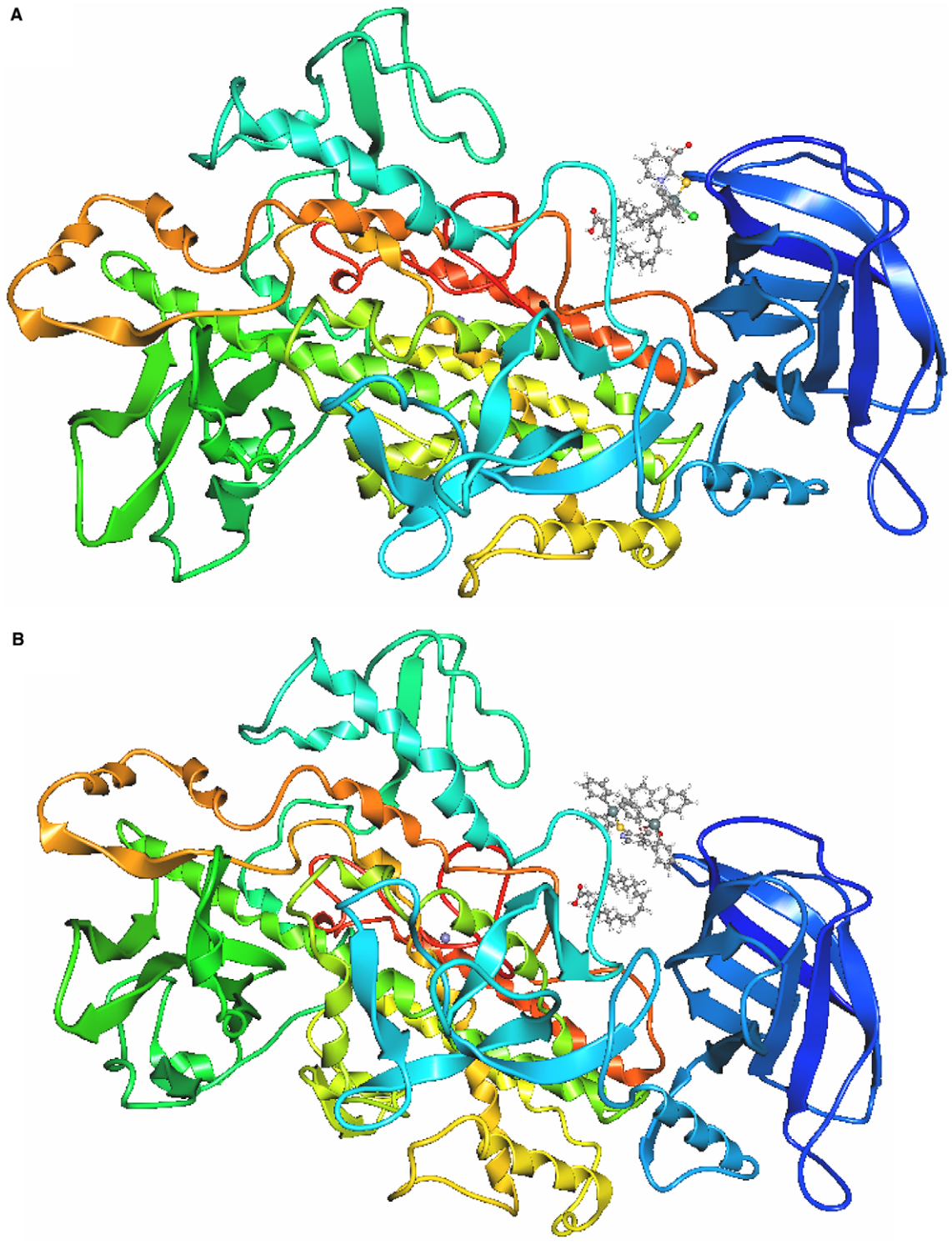

Fig. 6. Ribbon representation of the substrate and complexes **1** (A) and **2** (B) docked into the binding site of the enzyme LOX (**ESI**).

3. Conclusions

In conclusion two organotin(IV) compounds with the thioamide 2-mercapto-nicotinic acid, which adopt trigonal bibyramidal geometry around the metal center, were found to inhibit the catalytic oxidation of linoleic acid to hydroperoxy-linoleic acid by the enzyme lipoxygenase (LOX). The values of the inhibition degree for compounds **1** and **2** follow the dependence on the number of phenyl groups presented in the molecules, while the inhibitory mechanism is found to be a reversible mixed, which indicate that the inhibitor binds at a site away from the substrate binding site, causing a reduction in the catalytic rate.

4. Experimental

4.1. Materials and instruments

All solvents used were of reagent grade, while thioamides, organotin chlorides, boric acid, lipoxygenase and linoleic acid (Aldrich, Merk) were used with no further purification. Elemental analysis for C, H, N, and S were carried out with a Carlo Erba EA MODEL 1108. Infrared spectra in the region of 4000–370 cm^{-1} were obtained in KBr discs. Far-infrared spectra in the region of 700–30 cm^{-1} were obtained in polyethylene discs, with a Perkin–Elmer Spectrum GX FT-IR spectrometer. The ^{119}Sn Mössbauer spectra were collected at 80 and 85 K, with a constant acceleration spectrometer equipped with $CaSnO_3$ source kept at low temperature. The UV kinetics spectra were collected in a UV–Vis/NIR V570 instrument. Complex **2** was synthesized according to the procedure described earlier [5a,5b].

4.2. Preparation of complex [$(C_6H_5)_2SnCl(HMNA)$] (1)

A suspension of the 2-mercapto-nicotinic acid, 0.076 g, 0.5 mmol in distilled water (8 cm^3) was treated with a solution of KOH 1 N (1 cm^3, 1 mmol and a clear solution was formed). A solution of di-phenyltin(IV) di-chloride ($(C_6H_5)_2SnCl_2$) 0.344 g, 1 mmol in methanol (3 cm^3) was added to the previous one. A pale yellow resin precipitated immediately, which turned to powder precipitation after stirring for 180 min. The precipitation was filtered off, washed with 2–3 cm^3 of cold distilled water and dried in vacuo over silica gel. Colorless crystals of (**1**) suitable for X-ray analysis were formed by slow evaporation of a solution of dichloromethane.

(**1**) Yield: 30%; m.p. >300 °C;. Elemental analysis of the crystals; Found: C, 46.35; H, 3.01; N, 3.63, S, 6.50%, calculated for $C_{18}H_{14}ClNO_2SSn$: C, 46.75; H, 3.05; N, 3.03, S, 6.93%. IR (cm^{-1}): 3048m, 1693s, 1648m, 1590s, 1565s, 1534m, 1479vs, 1444m, 1431vs, 1390vs, 1129s, 1077vs, 1021s, 996vs, 766vs, 729vs, 693vs, 667m. far-IR (cm^{-1}): 383m, 342m, 318w, 292w, 282w, 272m, 239m, 220m, 205w, 198m, 151s, 121m, 103m. ^1H NMR d_6-DMSO (ppm): 8.51 (t, $^3J = 5$), 8.31 (s), 8.26 (s, $^2J(^{119}Sn–C–^1H) = 66$ Hz), 7.87 (d, $^3J = 7$), 7.70–7.22 (m). ^{13}C NMR d_6-DMSO (ppm): 165.5, 152.0, 139.2, 135.8, 134.8, 133.2, 129.3, 128.5, 128.0, 127.5, 120.9, 115.26.

4.3. Study of lipoxygenase inhibition mechanism

4.3.1. Preparation of solutions

The buffer used for all experiments was 0.2 M boric acid at pH 9: 0.1 mol boric acid (H_3BO_3, 6.18 g) was added to 300 cm^3 distilled water. The pH was adjusted to 9 with 50% w/v NaOH. Finally, the solution was diluted to 500 cm^3 [36a]. Linoleic acid substrate solution was prepared as described below: 0.05 cm^3 of linoleic acid was dissolved in 0.05 cm^3 95% ethanol in a volumetric flask (50 cm^3). The appropriate volume of H_2O was gradually added in the flask. 5 cm^3 of the prepared solution was added to 30 cm^3 of the borate buffer. Enzyme solution (lipoxygenase): a solution of 10 000 U of enzyme for each cm^3 of borate buffer was prepared in ice cold bath [36b]. An amount of 500 U for every 3 cm^3 of reaction mixture is used in every experiment. A unit of lipoxygenase causes and increase in absorption at 234 nm equal to 0.001 per minute.

4.3.2. Procedure

Enzyme activity was monitored by UV analysis. 0.05 cm^3 of enzyme solution was added to a cuvette containing 2 cm^3 linoleic acid solution and the appropriate amounts of buffer and inhibitor solutions in thermostatic water bath at 25 °C. There was no pre-incubation time of the enzyme with inhibitor solution. The activity of the enzyme was determined by monitoring the increase in the absorption caused by the oxidation of linoleic acid at 234 nm and 25 °C [36c] ($\varepsilon = 25\,000\ M^{-1}\ cm^{-1}$ [36d,36e]). Four standard solutions of complexes in DMSO (10^{-2}, 5×10^{-3}, 2.5×10^{-3}, 10^{-3} M) were used for the inhibition activity experiments (three sets). In this case, the substrate concentration was kept constant (0.3 mM), while the amounts of buffer and inhibitor solutions varied according to the inhibitor final concentration needed (5–60 μM or 9–18 μl from standard solutions). The total experiment volume was 3 cm^3.

For K_m and υ_{max} determination experiments (three sets of experiments), the concentration of inhibitor was kept constant (15 μM, 9 μl from a standard solution of 5×10^{-3} M in DMSO) and the substrate concentrations used were 0.01, 0.025, 0.05, 0.075 and 0.1 mM. All solutions were kept at thermostatic water bath at 25 °C, except from the enzyme solution that was kept at ice cold bath (0 °C).

4.4. Computational methods – docking study

The docking program used was ArgusLab [37a]. The programme was also utilized for the visualization and molecular modeling of the compounds. The three dimensional coordinates of lipoxygenase were obtained through the internet at the Research Collaboratory for Structural Bioinformatics (RCSB) Protein Data Bank [37b] and of the complexes by X-ray diffraction analysis [5a]. ArgusLab implements an efficient grid-based docking algorithm, which approximates an exhaustive search within the free volume of the binding site cavity. In order to explore the conformational space, the program performs a geometry optimization fit of the flexible ligand (rings are treated as rigid) along with incremental construction of the ligand's torsions. Thus, docking occurs between flexible ligands and a rigid protein. The orientation of the ligand is evaluated with a shape scoring function based on an enhancement of the XScore(HP) method of Wang and co-workers [37c] and final poses are ranked

by lowest interaction energy values. Prior to docking, ground state optimizations on the X-ray structures of the complexes were carried out using the PM3 parameterization scheme [37d] as implemented in the ArgusLab package in order to confirm no significant divergence in conformation of the complexes due to crystal packing effects.

4.5. X-ray structure determination

Data were collected by the ω scan technique in the range $4.86° < 2\theta < 24.71°$ on a KUMA KM4CCD four-circle diffractometer [38a] with CCD detector, using graphite-monochromated Mo Kα ($\lambda = 0.71073$ Å) at 293(2) K. Cell parameters were determined by a least-squares fit [38b]. All data were corrected for Lorentz-polarization effects and absorption [38b,38c].

The structure was solved with direct methods with SHELXS97 [38d] and refined by full-matrix least-squares procedures on F^2 with SHELXL97 [38e]. All non-hydrogen atoms were refined anisotropically, hydrogen atoms were located at calculated positions and refined as a 'riding model' with isotropic thermal parameters fixed at 1.2 times the U_{eq}'s of appropriate carrier atom. Significant crystal data are given below.

Compound **1**: $C_{18}H_{14}ClNO_2SSn$, $M_W = 474.51$, monoclinic in $P2_1/n$, $a = 15.089(3)$ Å, $b = 15.846(3)$ Å, $c = 16.691(3)$ Å, $\beta = 105.57(3)°$, $V = 3844.4(13)$ Å^3, $Z = 8$, $\rho(\text{cald}) = 1.640$ g cm^{-3}, $\mu = 1.588$ mm^{-1}, reflections collected 17 648, Final R^a, $wR_2{}^b$ [$I > 2\sigma(I)$] indices 0.0597 and = 0.1338, respectively. ($^aR = \sum\|F_o| - |F_c\|/\sum|F_o|$; $^bwR_2 = [\sum w(F_o^2 - F_c^2)^2/\sum w(F_o^2)^2]^{1/2}$).

5. Supplementary material

Crystallographic data for the structure reported in this paper have been deposited with the Cambridge Crystallographic Data Centre as Supplementary Publication Nos. CCDC-286987 **1**. Copies of the data can be obtained free of charge on application to CCDC, 12 Union Road, Cambridge CB2 1EZ, UK (fax: +44 1223 336 033; e-mail: deposit@ccdc.cam.ac.uk).

Acknowledgment

This research was co-funded by the European Union in the framework of the program "Heraklitos" of the "Operational Program for Education and Initial Vocational Training" of the 3rd Community Support Framework of the Hellenic Ministry of Education, funded by 25% from national sources and by 75% from the European Social Fund (ESF) and was carried out in partial fulfillment of the requirements for the Ph.D. Thesis of Miss MNX within the graduate program in Bioinorganic Chemistry. S.K.H. acknowledge Prof. K. Drainas and Assoc. Prof. A. Tselepis of the Laboratory of Biochemistry of the Department of Chemistry, University of Ioannina, for their useful discussions on lipoxygenase inhibition mechanism assignment.

References

[1] A.G. Davis, Organotin Chemistry, VCH, Verlagsgesellschaft, Weinheim, Germany, 1997.
[2] P.J. Smith, Chemistry of Tin, Blackie Academic and Professional an Imprint of Thomson Science, London, UK, 1998.
[3] L. Pellerito, L. Nagy, Coord. Chem. Rev. 224 (2002) 111.
[4] (a) K. Cain, M..D. Partis, D.E. Griffiths, Biochem. J. 166 (1977) 593;
(b) B.G Farrow, A.P. Dawson, Eur. J. Biochem. 86 (1978) 85.
[5] (a) M.N. Xanthopoulou, S.K. Hadjikakou, N. Hadjiliadis, M. Schürmann, K. Jurkschat, A. Michaelides, S. Skoulika, T. Bakas, J.J. Binolis, S. Karkabounas, C. Haralampopoulos, J. Inorg. Biochem. 96 (2003) 425;
(b) M.N. Xanthopoulou, S.K. Hadjikakou, N. Hadjiliadis, M. Schürmann, K. Jurkschat, J.J. Binolis, S. Karkabounas, C. Haralampopoulos, Bioinorg. Chem. Appl. 1 (2003) 227;
(c) C.T. Chasapis, S.K. Hadjikakou, A. Garoufis, N. Hadjiliadis, T. Bakas, M. Kubicki, Y. Ming, Bioinorg. Chem. Appl. 2 (2003) 43.
[6] M. Gielen, Coord. Chem. Rev. 151 (1996) 41.
[7] M. Nath, S. Pokharia, R. Yadav, Coord. Chem. Rev. 215 (2001) 99.
[8] M.D. Couse, G. Faraglia, U. Russo, L. Sindellari, G. Valle, J. Organomet. Chem. 513 (1996) 77.
[9] K.C. Molloy, T.G. Purcell, D. Cunningham, P. McCardle, T. Higgins, Appl. Organomet. Chem. 1 (1987) 119.
[10] J. Susperregui, M. Bayle, J.M. Leger, G. Deleris, J. Organomet. Chem. 556 (1998) 105.
[11] A. Paula, G. de Sousa, R.M. Silva, A. Cesar, J.L. Wardell, J.C. Huffman, A. Abras, J. Organomet. Chem 605 (2000) 82.
[12] J. Susperrgui, A. Petsom, M. Bayle, G. Lain, C. Giroud, T. Baltz, G. Deleris, Eur. J. Med. Chem. 32 (1997) 123.
[13] G. Domazetis, R.J. Magee, B.D. James, J.D. Cashion, J. Inorg. Nucl. Chem. 43 (1981) 1351.
[14] F. Huber, R. Schmiedgen, M. Schürmann, R. Barbieri, G. Ruisi, A. Silvestri, Appl. Organomet. Chem. 11 (1997) 869.
[15] M. Schürmann, F. Huber, Acta Crystallogr., Sect. C 50 (1994) 206.
[16] R. Schmiedgen, F. Huber, H. Preut, Acta Crystallogr., Sect. C 49 (1993) 1735.
[17] M. Castano, A. Macias, A. Castineiras, A.S. Gonzalez, E.G. Martinez, J. Casas, J. Sordo, W. Hiller, E. Castellano, J. Chem. Soc., Dalton Trans. (1990) 1001.
[18] L. Damude, P. Dean, V. Manivannan, R. Srivastava, J. Vittal, Can. J. Chem. 68 (1990) 1323.
[19] G. Valle, R. Ettorre, U. Vettori, V. Peruzzo, G. Plazzogna, J. Chem. Soc., Dalton Trans. (1987) 815.
[20] G. Domazetis, B.D. James, M.F. Mackay, R.J. Magee, J. Inorg. Nucl. Chem. 41 (1979) 1555.
[21] M. Masaki, S. Matsunami, H. Ueda, Bull. Chem. Soc. Jpn. 51 (1978) 3298.
[22] V. Berceanc, C. Crainic, I. Haiduc, M.F. Mahon, K.C. Molloy, M.M. Venter, P.J. Wilson, J. Chem. Soc., Dalton Trans. (2002) 1036.
[23] R. Schmiedgen, F. Huber, A. Silvestri, G. Ruisi, M. Rossi, R. Barbieri, Appl. Organomet. Chem. 12 (1998) 861.
[24] R. Schmiedgen, F. Huber, M. Schürmann, Acta Crystallogr., Sect. C 50 (1994) 391.
[25] L. Petrilli, F. Caruso, E. Rivarola, Main Group Met. Chem. 17 (1994) 439.
[26] R. Barbieri, E. Rivarola, F. Di Bianca, F. Huber, Inorg. Chim. Acta 57 (1982) 37.
[27] R. Barbieri, F. Di Bianca, E. Rivarola, F. Huber, Inorg. Chim. Acta 108 (1985) 141.

[28] R.A. Goyer, in: M.O. Amdur, J. Doull, C.D. Klaassen (Eds.), Casarett and Doull's Toxicology: The Basic Science of Poisons, Pergamon Press, New York, 1991, p. 629.
[29] (a) B. Samuelsson, S.E. Dahlen, J. Lindgren, C.A. Rouzer, C.N. Serhan, Science 237 (1987) 1171;
(b) M.J. Knapp, J.P. Klinman, Biochemistry 42 (2003) 11466.
[30] K.C. Molloy, T.G. Purcell, D. Cunningham, P. McCardle, T. Higgins, Appl. Organomet. Chem. 1 (1987) 119.
[31] (a) W. Jiazhu, H. Jingshuo, H. Liyiao, S. Dashuang, H. Shengzhi, Inorg. Chim. Acta 152 (1988) 67;
(b) M.D. Couce, G. Faraglia, U. Russo, L. Sindellari, G. Valle, J. Organomet. Chem. 513 (1996) 77.
[32] (a) R.V. Parish, in: G.J. Long (Ed.), Mossbauer Spectroscopy Applied to Inorganic Chemistry, Plenum Press, New York, 1984;
(b) G.M. Bancroft, R.H. Platt, Adv. Inorg. Chem. Radiochem. 15 (1972) 59.
[33] A.W. Addison, T. Nageswara Rao, J. Reedijk, J. van Rijk, G.C. Verschoor, J. Chem. Soc., Dalton Trans. (1984) 1349.
[34] P.V. Bychkov, T.N. Shekhovtsova, E.R. Milaeva, Bioinorg. Chem. Appl. 3 (2005) 191.
[35] I.H. Segel, Biochemical Calculations, second ed., Wiley, New York, 1976.
[36] (a) H. Theorell, S. Bergstrom, A. Akeson, Pharm. Acta Helv. 21 (1946) 318;
(b) A.L. Tappel, P.D. Boyer, W.O. Lumdberg, Arch. Biochim. Biophys. 42 (1953) 293;
(c) R.T. HolmanMethods of Biochemical Analysis, vol. 2, Interscience, New York, 1958, p. 113;
(d) J.M. Lopez-Nicolas, R. Bru, A. Sanchez-Ferrer, F. Carcia-Carmona, Anal. Biochem. 221 (1994) 410;
(e) B. Axelrod, T.M. Cheesbrough, S. Laakso, Method Enzymol. 71 (1981) 441.
[37] (a) ArgusLab. M.A. Thompson, Planaria Software, Seattle, WA 98155, 2005;
(b) Protein Data Bank. Available from: <http://www.rcsb.org/pdb/>;
(c) R. Wang, L. Lai, S.J. Wang, Comput. Aided Mol. Des. 16 (2002) 11–26;
(d) J.J.P. Stewart, J. Comput. Chem. 10 (1989) 210.
[38] (a) KUMA KM-4CCD user manual, KUMA Diffraction, Wroclaw, Poland, 1999;
(b) CRYSALIS, Program for Reduction of the Data from KUMA CCD Diffractometer, KUMA Diffraction, Wroclaw, Poland, 1999;
(c) R.H. Blessing, J. Appl. Crystallogr. 22 (1989) 396;
(d) G.M. Sheldrick, Acta Crystallogr., Sect. A 46 (1990) 467;
(e) G.M. Sheldrick, SHELXL-97, Program for the Refinement of Crystal Structures, University of Göttingen, Göttingen, Germany, 1997.